Environmental Science Advances

ROYAL SOCIETY OF CHEMISTRY

PAPER

View Article Online
View Journal | View Issue

Open Access Article. Published on 12 September 2025. Downloaded on 1/16/2026 10:05:29 AM.
This article is licensed under a Creative Commons Attribution-NonCommercial 3.0 Unported Licence.

Check for updates

Cite this: *Environ. Sci.: Adv.*, 2026, **5**, 118

Monolithic *vs.* particle-based solid-phase extraction for selective separation of lead from aqueous matrices

Pranta Sarker, †[a] Ismail Rahman, †*[b] Kouki Yunoshita,[a] M. Ferdous Alam,[bc] Yoshiaki Furusho,[d] Asami S. Mashio[e] and Hiroshi Hasegawa*[e]

Received 4th March 2025
Accepted 1st September 2025

DOI: 10.1039/d5va00057b

rsc.li/esadvances

Effective removal of trace lead (Pb) from waste matrices is crucial to meet stringent environmental regulations designed to mitigate toxicological risks and protect human health. This study investigates the efficacy of a monolithic solid-phase extraction (m-SPE) column for the selective separation of trace Pb from aqueous matrices, comparing its performance to conventional particle-packed solid-phase extraction (p-SPE) columns. Key operational parameters, including solution pH, flow rate, washing solvent, and eluent, were optimized to maximize Pb retention on both SPE columns. Potential interference from common matrix ions was investigated and found to be minimal. Furthermore, the presence of counter anions enhanced Pb^{2+} retention on the m-SPE column, likely by promoting the formation of ion pairs. Notably, the SPE columns demonstrated reusability over multiple cycles without significant loss of efficiency. The p-SPE and m-SPE columns demonstrated satisfactory Pb^{2+} retention while exhibiting minimal retention of common elements, as confirmed by analysis of certified reference river water with elevated contents of trace elements. The m-SPE column demonstrated enhanced performance compared to the p-SPE column due to its high permeability, low backpressure, and robust porosity. These characteristics resulted in enhanced selectivity, reproducibility, and overall efficiency in the preferential separation of trace Pb from environmental matrices.

Environmental significance

This study presents a novel approach for the selective separation of trace lead from complex industrial waste matrices using supramolecule-equipped monolithic SPE and compares its performance with traditional particle-based SPE. The work offers a potential solution for safeguarding water quality and mitigating toxicological risks. The findings have implications for improving compliance with environmental safety regulations and protecting human health.

1 Introduction

Lead (Pb), a potentially toxic element, poses significant threats to ecosystems and human health due to its pervasive presence, high toxicity, and persistent nature in the environment.[1,2] While naturally occurring Pb exists, anthropogenic sources, such as industrial emissions, ethnomedicinal practices, cosmetics, jewelry, toys, and food, are the primary contributors to environmental contamination.[3] Exposure to Pb can lead to various adverse health effects, primarily through increased oxidative stress, impacting the cardiovascular, hepatic, renal, reproductive, immune, and neurological systems.[4,5] Consequently, stringent regulations on Pb content in environmental matrices have been established.[6,7] For instance, the permissible concentration of Pb in drinking water is 10 μg L^{-1}.[8,9]

Several instrumental approaches, *e.g.*, graphite furnace atomic absorption spectrometry,[10] flame atomic absorption spectrometry,[11] inductively coupled plasma optical emission spectrometry (ICP-OES),[12,13] or inductively coupled plasma mass spectrometry (ICP-MS)[14] are available to measure Pb content in aqueous matrices. However, the quantification of Pb is often challenged by the low sensitivity of analytical instruments at trace concentrations and the interfering effects of matrix components.[15] To overcome these limitations, separation or preconcentration techniques are commonly employed prior to analysis.[16–18] Several methods are available for this purpose, including co-precipitation, ion exchange, liquid–liquid

[a]*Graduate School of Natural Science and Technology, Kanazawa University, Kakuma, Kanazawa 920-1192, Japan*

[b]*Institute of Environmental Radioactivity, Fukushima University, 1 Kanayagawa, Fukushima City, Fukushima 960-1296, Japan. E-mail: immrahman@ipc.fukushima-u.ac.jp*

[c]*Institute of Nuclear Science and Technology, Atomic Energy Research Establishment, Ganakbari, Savar, Dhaka 1349, Bangladesh*

[d]*GL Sciences Inc., 6-22-1 Nishi Shinjuku, Shinjuku-ku, Tokyo, 163-1130, Japan*

[e]*Institute of Science and Engineering, Kanazawa University, Kakuma, Kanazawa 920-1192, Japan. E-mail: hhiroshi@se.kanazawa-u.ac.jp*

† Co-first author.

© 2026 The Author(s). Published by the Royal Society of Chemistry

Open Access Article. Published on 12 September 2025. Downloaded on 1/16/2026 10:05:29 AM. This article is licensed under a Creative Commons Attribution-NonCommercial 3.0 Unported Licence.

extraction, cloud point extraction, micro-extraction, and solid-phase extraction (SPE).[19–25] Among these, SPE is often preferred due to its high sensitivity, simplicity, speed, low sample volume requirements, and environmentally friendly nature.[16,26]

The SPE is a widely used technique for separating and preconcentrating analytes from complex matrices. While SPE procedures utilizing chemical reactions[27,28] or functionalized solid supports[29,30] are common, they often struggle to recover trace levels of Pb in samples with high concentrations of other divalent transition or post-transition elements.[31] To address this, SPE sorbents with high selectivity, reusability, and efficient analyte recovery are needed.[32,33] One promising approach involves using 'supramolecules' – molecules capable of 'molecular recognition' – covalently attached to silica or polymeric supports.[26,34,35] These supramolecules selectively capture target analytes, such as Pb, through 'host–guest' interactions, enabling efficient separation even in complex matrices.[15,16,31,36] Although sorbents utilizing this crown ether technology have been applied for Pb^{2+} preconcentration in conventional particle-packed formats, this study provides the first systematic comparison of the sorbent's performance when engineered into a monolithic (m-SPE) *versus* a particle-packed (p-SPE) architecture. This direct evaluation of the column format's impact on key performance metrics like separation efficiency, throughput, and eluent consumption represents the primary novelty of this work.

The m-SPE utilizes a single, porous material, often composed of methacrylate polymers (*e.g.*, butyl-, lauryl-, octadecyl-, or 2-hydroxyethyl methacrylate).[37] These materials provide hydrophobicity suitable for reversed-phase SPE and offer advantages such as high capacity, porosity, and permeability. It makes m-SPE ideal for techniques like capillary electrophoresis and microfluidic applications.[38–40] Conversely, p-SPE employs a variety of sorbent materials packed into a column, including chemically bonded silica, graphitized carbon, ion-exchange materials, and molecularly imprinted polymers.[41,42] These sorbents offer diverse separation mechanisms, including affinity-based separation, and can be deployed in various formats (online, offline, on-column, *etc.*).[41–43] Ultimately, the choice between m-SPE and p-SPE depends on factors such as the sample matrix, analyte properties, and desired sensitivity.

This study presents the first reported comparison of supramolecule-equipped p-SPE and m-SPE for the non-destructive preferential separation of trace Pb from environmental matrices. The findings have potential applications in Pb separation and preconcentration from complex industrial waste matrices, contributing to improved compliance with environmental safety regulations.

2 Experimental

2.1 Materials

2.1.1 Reagents. All reagents used in this study were of analytical grade and used as received without further purification. A 1000 mg L^{-1} Pb standard solution and a multi-element standard solution containing Li, Na, Mg, K, Ca, Sr, Ba, and Fe (all at 1000 mg L^{-1}) were obtained from Kanto Chemical Co. (Tokyo, Japan). A separate multi-element standard solution (1000 mg L^{-1}) was purchased from Merck (Darmstadt, Germany). Ethylenediaminetetraacetic acid (EDTA) was procured as an eluent from Wako Pure Chemical (Osaka, Japan).

Various metal salts, including potassium chloride (KCl), sodium nitrate ($NaNO_3$), sodium perchlorate ($NaClO_4$), sodium acetate (CH_3COONa), sodium formate (HCOONa), sodium propionate ($C_3H_5NaO_2$), and sodium benzoate ($C_7H_5NaO_2$), along with nitric acid (HNO_3), hydrochloric acid (HCl), and sodium hydroxide (NaOH) were obtained from Kanto Chemical (Tokyo, Japan).

Buffer solutions (0.1 M) were prepared using acetic acid/sodium acetate (AcOH/AcONa) from Kanto Chemical Co. to maintain a pH of 3–5, 2-(*N*-morpholino)ethanesulfonic acid (MES) from Sigma-Aldrich (St. Louis, MO) for a pH of 6, 4-(2-hydroxyethyl)piperazine-1-ethanesulfonic acid (HEPES) from Nacalai Tesque (Kyoto, Japan) for a pH of 7–8, and tris(hydroxymethyl)methylamino-propanesulfonic acid (TAPS) from MP Biomedicals (Solon, OH) for a pH of 9–10.

2.1.2 Solid-phase extraction systems. The p-SPE and m-SPE columns were supplied by GL Sciences (Tokyo, Japan). A commercially available Pb-selective sorbent, AnaLig Pb-02, from IBC Advanced Technologies (American Fork, UT), is used to prepare the SPE columns. The proprietary sorbent utilizes a silica gel base support functionalized with a crown ether, and the sorption ability is attributable to molecular recognition and macrocyclic chemistry. The chemical structures and images of both SPE configurations are presented in Fig. S1 (Appendix A. SI).

2.1.3 Certified reference material. The performance of the p-SPE and m-SPE columns was validated using a certified reference material (CRM) for river water, NMIJ CRM 7202-c (trace elements in river water, elevated level), obtained from the National Metrology Institute of Japan (NMIJ).[44] This CRM was selected because it provides a complex, natural aqueous matrix with certified concentrations of numerous potential interfering ions, enabling a rigorous assessment of the method's selectivity and accuracy under environmentally relevant conditions. The certified and measured values of different elements in the NMIJ CRM 7202-c[44] are listed in Table S1 (Appendix A. SI).

2.1.4 Instrumentation. Solution metal ion concentrations were measured *via* inductively coupled plasma optical emission spectrometry (ICP-OES) using a Thermo Fisher Scientific iCAP 6300 instrument or inductively coupled plasma mass spectrometry (ICP-MS) using a PerkinElmer NexION 300S instrument (Waltham, MA). The surface morphology and internal structure of the Monolithic AnaLig Pb-02 column were characterized using a JEOL JSM-7100F field emission-scanning electron microscope (FE-SEM) (Tokyo, Japan) equipped with an Oxford Instruments energy-dispersive X-ray (EDX) spectroscopy detector (Oxfordshire, UK). Fourier Transform Infrared (FTIR) spectra were recorded using a JASCO FTIR-460 spectrometer (JASCO Corporation, Tokyo, Japan). Optimization experiments for Pb-separation were performed using a GL Sciences GL-SPE vacuum manifold kit (Tokyo, Japan) coupled with an AS ONE

Open Access Article. Published on 12 September 2025. Downloaded on 1/16/2026 10:05:29 AM.
This article is licensed under a Creative Commons Attribution-NonCommercial 3.0 Unported Licence.

CAS-1 air pump (Osaka, Japan). Solution pH values were measured with a Horiba Instruments Navi F52 pH meter (Kyoto, Japan). Ultrapure water (UPW) was generated by a Sartorius Stedim Biotech water purification system (Gottingen, Germany).

2.1.5 Laboratory wares. The following laboratory wares were used during the experimental steps: low-density polyethylene containers (Nalgene Nunc, Rochester, NY), screw-capped polyethylene tubes (AS ONE, Osaka, Japan), polypropylene jars (Tomiki Medical Instrument, Kanazawa, Japan), and micropipette tips (Nichiryo, Tokyo, Japan). All laboratory wares were subjected to a standardized cleaning protocol before use to eliminate potential contamination. The protocol consisted of an initial overnight soak in Scat 20X-PF detergent and subsequent overnight immersion in 4 M HCl. After each soaking step, the labware was thoroughly rinsed with UPW.

2.2 Methods

The efficiency of m-SPE and p-SPE systems for the selective separation of Pb^{2+} from aqueous matrices have been compared in terms of retention and recovery rates. The SPE protocol involved a series of steps: rinsing, conditioning, sample loading, washing, and elution. The retention rate was calculated as the ratio of Pb^{2+} moles in the elution effluent to the total moles in all effluents. In contrast, the recovery rate was determined by comparing the cumulative moles of Pb^{2+} recovered from all fractions (sample loading, wash, and elution) to the initial moles loaded.

Optimization of the m-SPE and p-SPE systems involved evaluating the influence of solution pH (1–6), flow rate (0.3–5 mL min^{-1}), washing solvent (acid or water), and eluent (EDTA; pH 4–9 and KCl). Fig. 1 shows a detailed schematic representation of the SPE-assisted protocol for separating target analytes from an aqueous waste matrix.

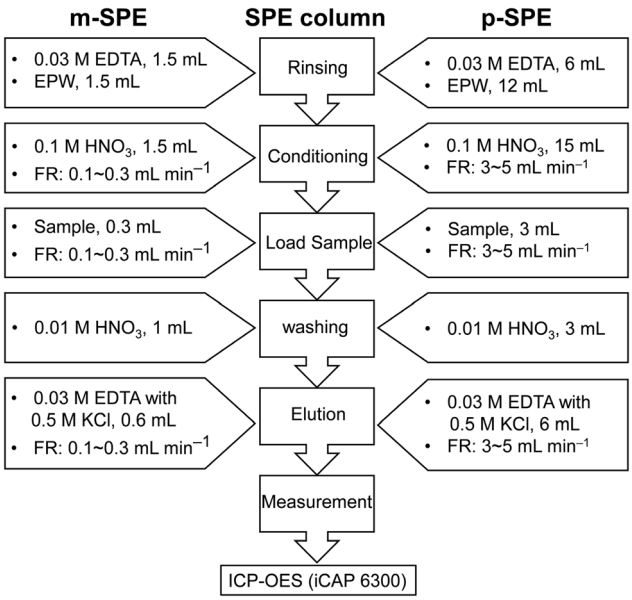

Fig. 1 Schematic representation of the SPE-assisted separation protocol.

To determine the maximum retention capacity (mmol g^{-1}) of both systems, Pb^{2+} solution (1.5 mM) at pH 1 was passed through the SPE columns until saturation. The influence of matrix cations (Li^+, Na^+, Mg^{2+}, Ca^{2+}, K^+, Sr^{2+}, Ba^{2+}, and Fe^{2+}; 0.001–1 M) on Pb^{2+} retention was investigated at pH 1. The effect of coexisting anions was examined using 0.01 M solutions of $NaNO_3$, $NaClO_4$, $C_2H_3NaO_2$, HCOONa, $C_3H_5NaO_2$, and $C_7H_5NaO_2$ in H_2O at pH 6. Further experiments evaluated the impact of varying concentrations (0.01–0.12 M) of $NaNO_3$, $NaClO_4$, and $C_2H_3NaO_2$ on Pb^{2+} retention. A 100 μM Pb^{2+} solution was used as a control in all these experiments. All solutions were equilibrated for 24 h prior to analysis, and all experiments were performed in triplicate.

To assess the acid resistance of AnaLig Pb-02, 10 mg of the sorbent was suspended in 10 mL of solution (pH ≈ 1.0) and agitated at 25 °C using a temperature-controlled shaker. Aliquots were collected after 3, 6, 12, and 24 h of contact, and the supernatants were analyzed using ICP-OES for silicon quantification.

FTIR spectroscopy was employed to characterize the sorbent before and after Pb^{2+} sorption. Spectra were recorded using the KBr pellet method in the range of 400–4000 cm^{-1}. EDX spectroscopy was also conducted to confirm Pb^{2+} uptake on the sorbent surface.

3 Results and discussion

3.1 Morphological features of the monolithic SPE material

Although the AnaLig Pb-02 sorbent is a commercial product, FE-SEM and EDX analyses were conducted to visually confirm and illustrate the continuous, interconnected porous network that defines the monolithic format. This direct visualization is crucial for interpreting the observed performance differences between the two SPE systems. The FE-SEM and EDX analysis of the monolithic silica material (Fig. 2) reveal a highly interconnected porous network with a large surface area. This intricate morphology is characterized by a continuous and uniform porous structure, as shown in the FE-SEM images (Fig. 2b and c), which facilitates efficient mass transfer and high permeability. EDX spectra analysis (Fig. 2d) confirms the elemental composition and purity of the silica, indicating minimal contamination and high chemical stability. Quantitative data on the material's high specific surface area and hierarchical pore structure are provided in Table S2 (Appendix A. SI), confirming the structural advantages that support its performance.

Such a unique surface structure offers several advantages for analytical separation applications. The high surface area enhances the interaction between analytes and the stationary phase, leading to improved separation efficiency. Additionally, the material's porosity supports higher sample loading capacities. The interconnected porous network reduces backpressure, enabling faster flow rates and shorter analysis times.[45,46] The robust and chemically stable nature of the monolithic silica material ensures consistent performance, making it highly effective for analytical separations.

 © 2026 The Author(s). Published by the Royal Society of Chemistry

Open Access Article. Published on 12 September 2025. Downloaded on 1/16/2026 10:05:29 AM.
This article is licensed under a Creative Commons Attribution-NonCommercial 3.0 Unported Licence.

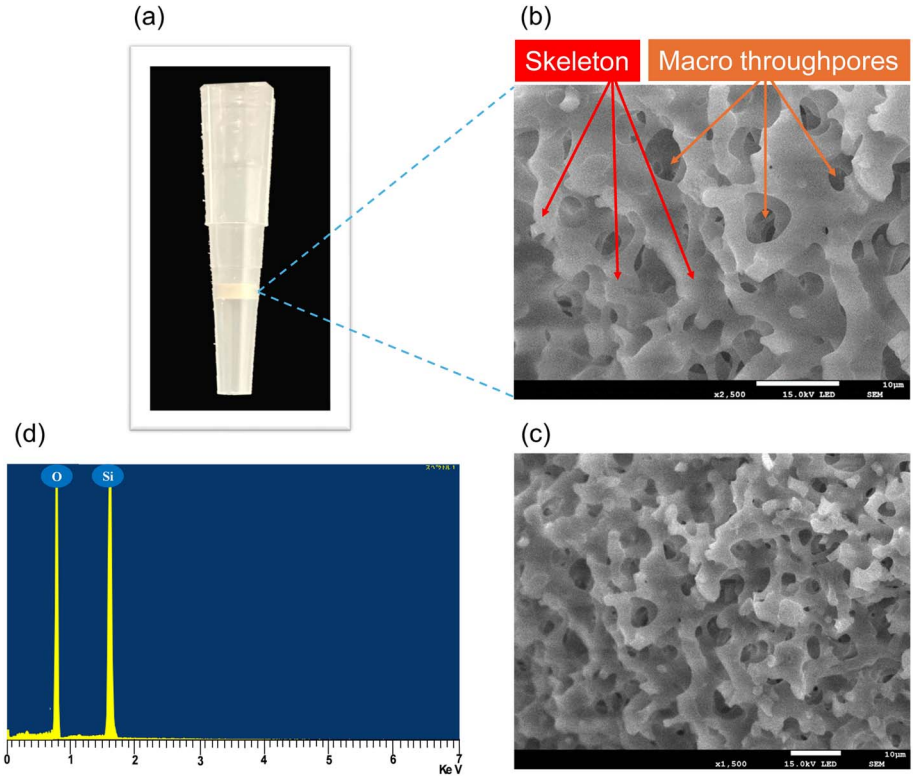

Fig. 2 (a) AnaLig Pb-02 monolithic column (m-SPE); (b) FE-SEM image at 2500× magnification; (c) FE-SEM image at 1500× magnification; (d) EDX spectrum of the m-SPE.

3.2 Pb-retention behavior: m-SPE *vis-à-vis* p-SPE

3.2.1 Effect of solution pH. The ionization state of metal ions and macrocycle functional groups is significantly influenced by solution pH, directly impacting the selectivity and efficiency of separation processes.[47] This study investigated the effect of solution acidity on Pb^{2+} retention rates in both m-SPE and p-SPE, examining a range of pH values (Fig. 3). Results indicated nearly quantitative Pb^{2+} retention in the acidic pH range by both SPE types. The data trend suggests that the MRT materials possess a high affinity for Pb^{2+}, with minimal influence from solution pH. However, at higher pHs, the SPEs exhibit a slight decrease in retention capacity, which may be due to the hydroxylation-induced precipitation.[25,48] Nevertheless, to avoid potential precipitation during sample preparation and prevent analyte binding to the silica gel support, a sample pH of 1 or lower was maintained for all subsequent experiments.

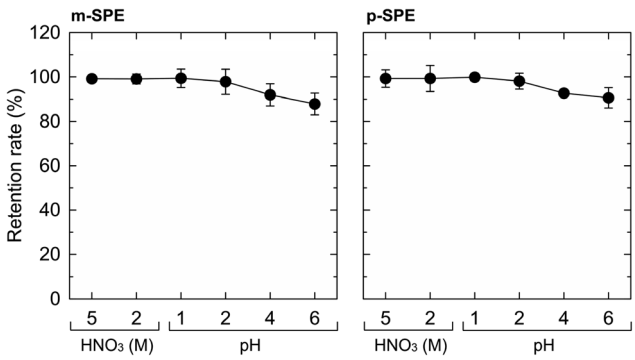

Fig. 3 Retention of Pb^{2+} in m-SPE and p-SPE as a function of solution acidity ($n = 3$). Experimental conditions: sample solution, 100 μM Pb^{2+}; matrix, H_2O; solution acidity, HNO_3 (2 and 5 M) and solution pH, 1–6; sample volume, 0.3 mL (m-SPE) and 3 mL (p-SPE); conditioning solution, HNO_3 (0.1 M); flow rate, ≤0.3 mL min^{-1} (m-SPE) and 3 mL min^{-1} (p-SPE).

The structural stability of the silica-based sorbent under these acidic conditions was confirmed by leaching tests, which showed no detectable silicon dissolution (see Table S3; Appendix A. SI).

3.2.2 Effect of washing solvents. The selection of an appropriate washing solvent in SPE procedures significantly influences both analyte recovery and the elimination of interfering compounds.[49] An optimal solvent enhances the selectivity and sensitivity of the method by removing unwanted matrix components while retaining target analytes.[26] This study demonstrates the superior efficacy of 0.01 M HNO_3 as a washing solvent compared to UPW. Washing with UPW resulted in a back-extraction of approximately 4 ± 0.7% Pb^{2+}, whereas no detectable back-extraction was observed with 0.01 M HNO_3. This difference can be attributed to the lower pH of HNO_3 (pH ∼ 2 or less) compared to UPW, underscoring the pH-dependent nature of selective retention in SPE.[15] These findings highlight the effectiveness of 0.01 M HNO_3 as the optimal washing solvent for subsequent stages of the procedure, ultimately leading to improved analytical performance.

Open Access Article. Published on 12 September 2025. Downloaded on 1/16/2026 10:05:29 AM.
This article is licensed under a Creative Commons Attribution-NonCommercial 3.0 Unported Licence.

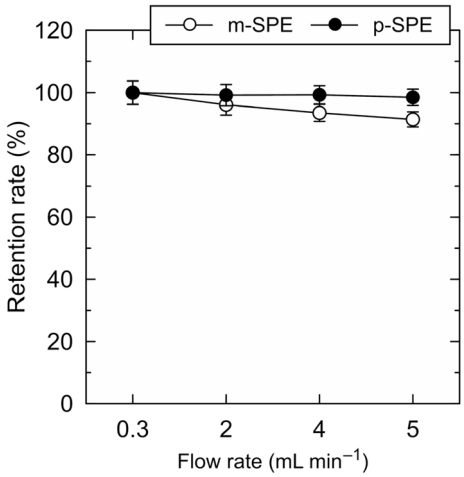

Fig. 4 Effect of flow rate on Pb^{2+} retention in m-SPE and p-SPE (n = 3). Experimental conditions: sample solution, 100 μM Pb^{2+} in H_2O; solution pH, 1; sample volume, 0.3 mL (m-SPE) and 3 mL (p-SPE); conditioning solution, 0.1 M HNO_3; flow rate, 0.3–5 mL min^{-1}.

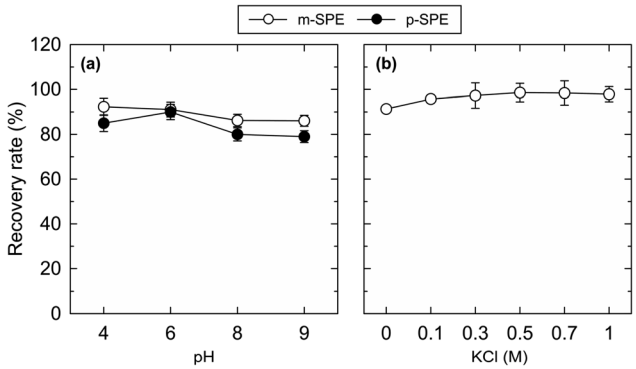

Fig. 5 Recovery of Pb^{2+} from m-SPE and p-SPE (n = 3). (a) Effect of eluent pH on the recovery rate (0.03 M EDTA; pH 4–9). (b) Effect of KCl concentration on the recovery rate (0.03 M EDTA with KCl; KCl concentration: 0.1–1 M). Experimental conditions: sample solution, 100 μM Pb^{2+}; matrix, H_2O; sample volume, 0.3 mL (m-SPE) and 3 mL (p-SPE); conditioning solution, 0.1 M HNO_3; eluent volume, 0.6 mL (m-SPE) and 6 mL (p-SPE); flow rate, ≤0.3 mL min^{-1} (m-SPE) and 3 mL min^{-1} (p-SPE).

3.2.3 Effect of flow rates. The influence of flow rate on the retention behavior of Pb^{2+} in m-SPE compared to p-SPE has been investigated. Flow rates were varied from 0.3 to 5 mL min^{-1} under optimized conditions. As illustrated in Fig. 4, m-SPE achieved quantitative Pb^{2+} extraction at a flow rate of 0.3 mL min^{-1}. However, Pb^{2+} retention gradually decreased with increasing flow rate, exhibiting 96, 93, and 91% retention at 2, 4, and 5 mL min^{-1}, respectively. Flow rates exceeding 5 mL min^{-1} were not attainable in the m-SPE system. The observed retention at higher flow rates in m-SPE is attributed to its continuous, porous structure, which minimizes backpressure and facilitates efficient mass transfer,[45] Such an inherent structural advantage allows for expedited sample processing without compromising analyte retention capacity. Conversely, p-SPE maintained slightly higher retention across the tested flow rates up to 5 mL min^{-1}. It indicates that quantitative extraction was achievable with p-SPE without a significant impact from increased flow rates.

3.2.4 Effect of eluents on recovery. Ethylenediaminetetraacetic acid (EDTA), an aminopolycarboxylate chelator, is recommended as an eluent for AnaLig Pb-02 MRT-SPE due to the high stability constant of the Pb–EDTA complex.[15,16] To optimize the elution procedure, the effect of pH on Pb^{2+} recovery using 0.03 M EDTA was investigated across a range of pH 4–9. EDTA exhibits limited solubility below pH 3,[50] thus precluding its use in highly acidic conditions.

As illustrated in Fig. 5a, Pb^{2+} recovery was approximately 92% between pH 4 and 6. The conditional formation constant of the Pb–EDTA complex increases with increasing pH, leading to improved recovery within this range.[51] However, recovery decreased at pH 8–9. Such a decline is attributed to the competitive formation of Pb-hydroxide species, which hinders Pb–EDTA complexation and subsequent elution by EDTA.[52]

To further enhance recovery, KCl was added to the eluent at concentrations ranging from 0.1 to 1 M. The addition of KCl significantly improved the recovery rate (Fig. 5b). Quantitative recovery was achieved using a mixed solution of 0.03 M EDTA with 0.5 M KCl at pH 6. Such an improvement is likely due to the combined effects of KCl-mediated ion substitution and EDTA-induced complexation reactions with Pb^{2+}.

Evaluation of eluent volume efficiency revealed that 6 mL of the optimized eluent (0.03 M EDTA with 0.5 M KCl; pH 6) was necessary for complete Pb^{2+} recovery with p-SPE. In contrast, only 0.6 mL eluent was required for m-SPE. Such a difference highlights the superior efficiency of m-SPE in terms of eluent consumption and cost-effectiveness for quantitative Pb^{2+} recovery.

In this analytical context, 'recovery' refers to the quantitative elution of the analyte from the column for measurement; the resulting Pb–EDTA eluent is collected and managed as hazardous waste according to institutional protocols.

3.2.5 Retention capacity and reusability. Retention capacity, an indicator of the stability of SPE systems, can be quantified by analyzing analyte content and breakthrough volume (BV).[53] The retention capacities of m-SPE and p-SPE systems were compared using 1.5 mM Pb^{2+} solutions at pH 1 under optimized conditions. Retention capacity was expressed as millimoles of analyte retained per gram of SPE material.

Results (Fig. 6) showed that retention capacity increased with sample volume for both systems, reaching saturation at 4 mL for m-SPE and 162 mL for p-SPE. Maximum retention capacities were 0.17 and 0.14 mmol g^{-1} for m-SPE and p-SPE, respectively. The higher retention capacity of m-SPE is attributed to its continuous porous structure, which provides a larger surface area and better flow characteristics, leading to enhanced analyte interaction.[46,54]

Regarding reusability, the Pb-02 MRT-SPE system demonstrated exceptional performance, maintaining analytical capabilities for over 100 retention–elution cycles. Such durability stems from the incorporation of macrocycles attached to solid supports within the SPEs, enabling selective analyte separation and repeated macrocycle use.[55]

 © 2026 The Author(s). Published by the Royal Society of Chemistry

Open Access Article. Published on 12 September 2025. Downloaded on 1/16/2026 10:05:29 AM.
This article is licensed under a Creative Commons Attribution-NonCommercial 3.0 Unported Licence.

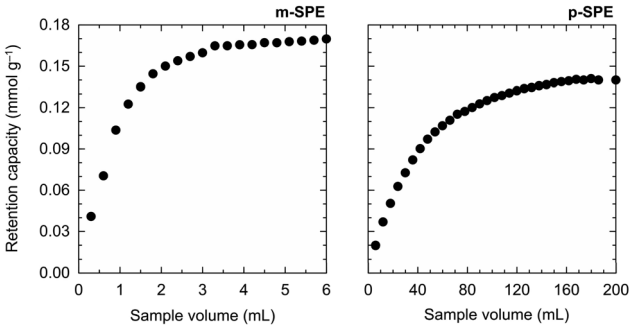

Fig. 6 Pb^{2+} retention capacity of m-SPE and p-SPE. Experimental conditions: 1.5 mM Pb^{2+} solution in H_2O; solution pH, 1; sample volume, 0.2–6 mL (m-SPE) and 6–200 mL (p-SPE); conditioning solution, 0.1 M HNO_3; flow rate, ≤0.3 mL min^{-1} (m-SPE) and 3 mL min^{-1} (p-SPE).

3.3 Interference studies

3.3.1 Effect of coexisting cations. The prevalence of alkaline and alkaline earth metal cations in aqueous environments raises concerns about their potential to compete with target metal ions for binding sites on solid-phase extraction (SPE) materials.[32] Therefore, a series of experiments was performed to evaluate the selectivity of the Pb-02 MRT-SPE material for Pb^{2+} in the presence of high concentrations of common competing cations.

Solutions containing 100 μM Pb^{2+} were spiked with varying concentrations (0.001–1 M) of individual cations (Li^+, Na^+, K^+, Mg^{2+}, Ca^{2+}, Fe^{2+}, Sr^{2+}, and Ba^{2+}). These solutions were processed using the MRT-SPE system under optimized conditions. The results (Fig. 7) indicated that Pb^{2+} retention remained above 98% even in the presence of 1 M concentrations of Li^+, Na^+, Mg^{2+}, Ca^{2+}, and Fe^{2+}. However, a decrease in Pb^{2+} retention efficiency (82–87%) was observed in the presence of 0.1 M K^+ and Sr^{2+} and 0.001 M Ba^{2+}. This reduced retention is likely due to the strong affinity of the Pb-02 MRT-SPE column for Sr^{2+} and Ba^{2+}, as the sorbent is designed to selectively capture metal ions based on charge and ionic radius.[26] The sorbent is designed to selectively separate and concentrate Pb^{2+} ions, and thus exhibits high selectivity for metals with ionic radii close to Pb^{2+} (1.33 Å). Ionic radii of different ions[56,57] are provided in Table S4 (Appendix A. SI). Sr^{2+}, with an ionic radius of 1.32 Å, showed quantitative retention, supporting the system's design criteria. Conversely, Ba^{2+} (ionic radius approximately 0.15 Å larger than Pb^{2+}) was also extracted. This may be due to the presence of multiple adsorption sites within the sorbent material.[26] While K^+ is a common constituent of natural waters, Sr^{2+} and Ba^{2+} are typically present only in trace amounts.[15] Consequently, the impact of the major ions commonly found in aqueous matrices on the selective separation of Pb^{2+} using this system is expected to be minimal.

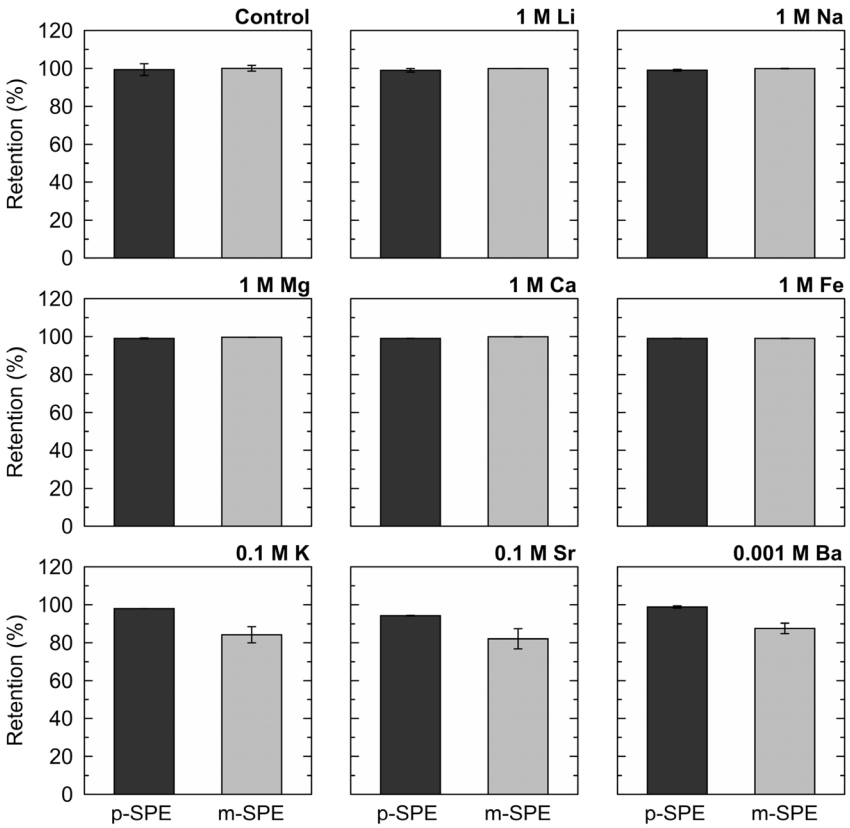

Fig. 7 Effect of coexistence cations on the Pb-retention in m-SPE and p-SPE ($n = 3$). Experimental conditions: sample solution, 100 μM Pb^{2+}; ion concentration, 0.001–0.1 M; matrix, H_2O; solution pH, 1; sample volume, 0.3 mL (m-SPE) and 3 mL (p-SPE); conditioning solution, 0.1 M HNO_3; flow rate, ≤0.3 mL min^{-1} (m-SPE) and 3 mL min^{-1} (p-SPE).

Open Access Article. Published on 12 September 2025. Downloaded on 1/16/2026 10:05:29 AM.
This article is licensed under a Creative Commons Attribution-NonCommercial 3.0 Unported Licence.

3.3.2 Effect of counter anions. To investigate the influence of counter anions on Pb^{2+} retention, various anions (0.01 M) were introduced to 100 μM Pb^{2+} solutions maintained at pH 6 (Fig. 8a). In the absence of added anions (control with 100 μM Pb^{2+} only), the Pb^{2+} retention rate was 74%. Notably, the addition of any anion enhanced retention rates. Nitrate and formate yielded 84 and 88% retention rates, respectively, while propionate increased the rate to 91%. The highest retention rates, approaching 100%, were observed with acetate, perchlorate, and benzoate ions.

Such variation can be rationalized by considering the Hofmeister series, which categorizes ions based on their ability to disrupt water structure and engage in ion-pairing or hydrophobic interactions.[58,59] In this series, chaotropic anions (*e.g.*, perchlorate, acetate, benzoate) are weakly hydrated and highly polarizable, promoting stronger ion pairing with Pb^{2+} due to reduced competition from water molecules. In contrast, kosmotropic anions (*e.g.*, nitrate, formate) are intensely hydrated and less prone to such interactions.[60,61] Larger anions (Table S5, see Appendix A. SI) such as perchlorate, acetate, and benzoate[62,63] demonstrated higher retention compared to smaller anions like nitrate. This trend is attributed to the enhanced ability of bulkier, chaotropic anions to form neutral or weakly charged ion pairs with Pb^{2+}, which are more readily retained by the sorbent through hydrophobic association and reduced hydration shielding.[64,65]

Furthermore, anion concentration significantly impacted Pb^{2+} retention (Fig. 8b). Higher anion concentrations led to quantitative extraction of Pb^{2+}. For instance, increasing the nitrate concentration resulted in a corresponding increase in Pb^{2+} retention, with complete extraction achieved at concentrations above 0.04 M. The degree of anion dissociation also played a role. Strong acids like perchloric acid, which fully dissociate, contributed to higher ion concentrations and improved retention compared to weak acids like formic acid, which only partially dissociate. These results demonstrate that both the size and concentration of counter anions are critical factors in enhancing Pb^{2+} retention within the m-SPE column.

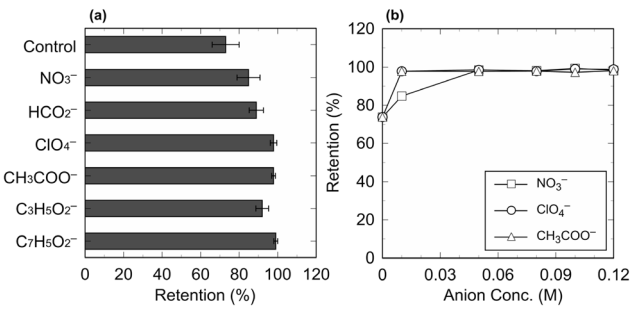

Fig. 8 (a) Impact of matrix anion on the Pb-retention; (b) impact of anion concentrations on the Pb-retention in m-SPE ($n = 3$). Experimental conditions: sample solution, 100 μM Pb^{2+}; ion concentration, 0.01 M (in experiment a) and 0.01–0.12 M (in experiment b); matrix, H_2O; solution pH, 6; sample volume, 0.3 mL (m-SPE) and 3 mL (p-SPE); conditioning solution, 0.1 M HNO_3; flow rate, ≤0.3 mL min^{-1} (m-SPE) and 3 mL min^{-1} (p-SPE).

3.4 Mechanism

Interpretation of the results necessitates a clear understanding of the metal separation mechanisms within the selected MRT-SPE column. While further research is needed to fully elucidate the mechanism of the MRT-SPE AnaLig Pb-02 column, a proposed model (Fig. 9), based on established SPE systems with immobilized macrocycles,[66] describes a non-destructive, selective metal separation. MRT-SPE employs macrocyclic ligands (*e.g.*, crown ethers) immobilized on supports (*e.g.*, silica gel, polymers).[26] Selective separation is achieved *via* molecular recognition, where the macrocyclic "host" preferentially binds specific metal ion "guests." Ionic size, charge, electronic interactions, and conformation of the macrocycle influence metal ion retention.[26,66] Binding occurs within the macrocyclic cavity or within three-dimensional cavity-like structures formed with associated sidearms.[26] This mechanism's effectiveness at low concentrations and in complex matrices makes MRT-SPE valuable for preconcentration and purification. Separation efficiency is also significantly impacted by macrocycle–solvent interactions and support material wettability. Unlike traditional solvent extraction, MRT-SPE is non-destructive, enabling repeated macrocycle use.[33]

To provide experimental support for this host–guest model, the sorbent was analyzed before and after Pb^{2+} uptake using FTIR and EDX spectroscopy (see Fig. S2, Appendix A. SI). The FTIR spectra were characterized by broad bands in the 3500–3400 cm^{-1} region, which are assigned to the –OH stretching vibrations of surface Si–OH groups, and a strong absorption band between 1100–1250 cm^{-1}, corresponding to Si–O–Si asymmetric stretching vibrations.[67,68] After Pb^{2+} sorption, no significant shifts or new peaks were observed. This lack of spectral change is consistent with the proposed molecular recognition mechanism, where the Pb^{2+} ion, the 'guest', is captured within the macrocyclic cavity, the 'host' without forming strong covalent bonds that would alter the vibrational modes of the host molecule. These findings agree with previous reports on metal–crown ether interactions.[16,26] The successful sorption of Pb^{2+} was then unequivocally confirmed by EDX analysis, which showed distinct peaks corresponding to Pb after the separation process.

3.5 Validation with CRM

Fig. 10 shows the comparative percentage retention of various elements in the NMIJ CRM 7202-c (as detailed in Table S1, see Appendix A. SI) for p-SPE and m-SPE. While both SPE types exhibited minimal retention of common elements within the certified river water samples, they competitively retained Rb, Sr, Se, along with Pb. As anticipated from the interference studies, the sorbent showed co-retention of Sr, which has an ionic radius nearly identical to that of Pb^{2+}. The partial retention of other ions like Rb and Se suggests secondary interactions may also occur within the complex CRM matrix. Nonetheless, the retention of Pb^{2+} remained significantly higher than that of most other elements, demonstrating the method's strong preference for the target analyte.

 © 2026 The Author(s). Published by the Royal Society of Chemistry

Open Access Article. Published on 12 September 2025. Downloaded on 1/16/2026 10:05:29 AM.
This article is licensed under a Creative Commons Attribution-NonCommercial 3.0 Unported Licence.

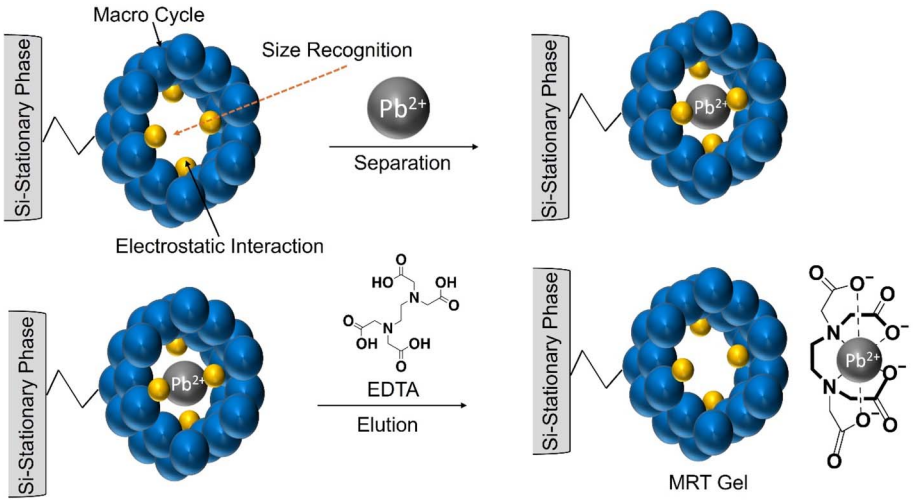

Fig. 9 A schematic illustration of the selective separation of Pb^{2+} by AnaLig Pb-02 MRT-SPE system.

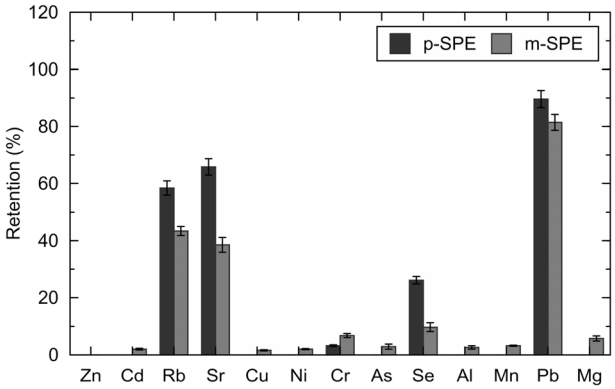

Fig. 10 Comparative percentage retention of elements present in NMIJ CRM 7202-c by p-SPE and m-SPE.

While the p-SPE system exhibited a slightly higher absolute retention of Pb^{2+} (~90%) compared to the m-SPE system (~82%), a more critical measure of performance in complex matrices is selectivity—the ability to isolate the target analyte from interfering ions. The m-SPE system demonstrated significantly greater selectivity for Pb^{2+} over co-retained elements like Sr(II). For instance, the selectivity factor (α) for Pb^{2+} over Sr(II) was calculated for both systems. The m-SPE system achieved a selectivity factor of approximately 2.16 (82% Pb/38% Sr), whereas the p-SPE system's factor was only 1.38 (90% Pb/65% Sr). This superior selectivity highlights the m-SPE format's enhanced ability to preferentially bind Pb^{2+} even in the presence of competing ions with similar chemical properties, reinforcing its suitability for selective separation from complex environmental matrices.

4 Conclusions

The selective separation of Pb^{2+} from aqueous waste matrices using SPE systems of particle-based (p-SPE) and monolithic (m-SPE) formats has been investigated. Optimal Pb^{2+} extraction was achieved using the m-SPE column under the following conditions: a pH range of 1–6, 0.10 M nitrate ion in the sample matrix, a sample loading flow rate of 0.3 mL min^{-1}, and an eluent solution of 0.03 M EDTA with 0.5 M KCl at pH 6. In contrast, the p-SPE column required a sample loading flow rate of 3 mL min^{-1} and an elution volume of 6 mL while maintaining the same pH range and eluent composition as the m-SPE column. The maximum retention capacities for the m-SPE and p-SPE columns were determined to be 0.17 and 0.14 mmol g^{-1}, respectively. These results indicate that the m-SPE column performs better in the highly selective separation of Pb^{2+} from complex waste solutions. Furthermore, the MRT-SPE method demonstrated minimal interference from common ions present in aqueous matrices. The presence of counter anions in the sample matrix enhanced Pb^{2+} retention on the m-SPE column, likely due to the formation of ion pairs, thereby improving the efficiency of the separation process. Notably, the m-SPE exhibited greater preference for Pb compared to the p-SPE, despite competitive retention of Rb, Sr, and Se from the CRM matrix. An additional advantage of the SPE column was its facile regeneration process, enabling multiple uses without significant loss of analytical performance. From a practical and cost-effectiveness standpoint, the m-SPE system demonstrates significant advantages. While this study focused on analytical-scale preconcentration, the high reusability (>100 cycles), faster sample processing potential, and ten-fold reduction in eluent consumption suggest it holds considerable promise for larger-scale, continuous separation processes. These factors contribute to lower operational costs and reduced chemical waste generation. Future work should focus on validating the method's performance with authentic industrial effluents, and pilot-scale testing would be required to confirm its economic feasibility.

Conflicts of interest

The authors declare that they have no known competing financial interests or personal relationships that could have appeared to influence the work reported in this paper.

Open Access Article. Published on 12 September 2025. Downloaded on 1/16/2026 10:05:29 AM.
This article is licensed under a Creative Commons Attribution-NonCommercial 3.0 Unported Licence.

Data availability

Backup experimental data are available from the corresponding author(s) upon reasonable request.

All data generated or analyzed during this study are included in this article and its SI. See DOI: https://doi.org/10.1039/d5va00057b.

Acknowledgements

The research was supported by Grants-in-Aid for Scientific Research (25H01197 (HH) and 24K15337 (IMMR)) from the Japan Society for the Promotion of Science (JSPS) and research grants from the Environmental Radioactivity Research Network Center (ERAN: P-24-27) at Fukushima University, Japan. While preparing this work, the authors used Gemini Advanced and Grammarly to paraphrase and edit the language. After using those tools, the authors reviewed and revised the content as needed and take full responsibility for the publication's content.

References

1 K. Kumar and D. Singh, Toxicity and bioremediation of the lead: A critical review, *Int. J. Environ. Health Res.*, 2024, **34**, 1879–1909.
2 B. Li, J.-Z. Guo, J.-L. Liu, L. Fang, J.-Q. Lv and K. Lv, Removal of aqueous-phase lead ions by dithiocarbamate-modified hydrochar, *Sci. Total Environ.*, 2020, **714**, 136897.
3 E. Obeng-Gyasi, Sources of lead exposure in various countries, *Rev. Environ. Health*, 2019, **34**, 25–34.
4 G. C. Mandal, A. Mandal and A. Chakraborty, The toxic effect of lead on human health: A review, *Hum. Biol. Public Health*, 2023, **3**, 1–11.
5 V. Matović, A. Buha, D. Đukić-Ćosić and Z. Bulat, Insight into the oxidative stress induced by lead and/or cadmium in blood, liver and kidneys, *Food Chem. Toxicol.*, 2015, **78**, 130–140.
6 P. Jarvis and J. Fawell, Lead in drinking water – An ongoing public health concern?, *Curr. Opin. Environ. Sci. Health*, 2021, **20**, 100239.
7 R. J. Santucci and J. R. Scully, The pervasive threat of lead (Pb) in drinking water: Unmasking and pursuing scientific factors that govern lead release, *Proc. Natl. Acad. Sci. U. S. A.*, 2020, **117**, 23211–23218.
8 World Health Organization, *Guidelines for Drinking-Water Quality: Fourth Edition Incorporating First Addendum*, World Health Organization, Geneva, 2017.
9 I. M. M. Rahman, S. Barua, R. Barua, R. Mutsuddi, M. Alamgir, F. Islam, Z. A. Begum and H. Hasegawa, Quality assessment of the non-carbonated bottled drinking water marketed in Bangladesh and comparison with tap water, *Food Control*, 2017, **73**, 1149–1158.
10 M. Aghamohammadi, M. Faraji, P. Shahdousti, H. Kalhor and A. Saleh, Trace determination of lead, chromium and cadmium in herbal medicines using ultrasound-assisted emulsification microextraction combined with graphite furnace atomic absorption spectrometry, *Phytochem. Anal.*, 2015, **26**, 209–214.
11 S. K. Wadhwa, M. Tuzen, T. G. Kazi, M. Soylak and B. Hazer, Polyhydroxybutyrate-b-polyethyleneglycol block copolymer for the solid phase extraction of lead and copper in water, baby foods, tea and coffee samples, *Food Chem.*, 2014, **152**, 75–80.
12 E. Durduran, H. Altundag, M. Imamoglu, S. Z. Yıldız and M. Tuzen, Simultaneous ICP-OES determination of trace metals in water and food samples after their preconcentration on silica gel functionalized with N-(2-aminoethyl)-2,3-dihydroxybenzaldimine, *J. Ind. Eng. Chem.*, 2015, **27**, 245–250.
13 R. N. C. S. Carvalho, G. B. Brito, M. G. A. Korn, J. S. R. Teixeira, F. d. S. Dias, A. F. Dantas and L. S. G. Teixeira, Multi-element determination of copper, iron, nickel, manganese, lead and zinc in environmental water samples by ICP OES after solid phase extraction with a C18 cartridge loaded with 1-(2-pyridylazo)-2-naphthol, *Anal. Methods*, 2015, **7**, 8714–8719.
14 H. Peng, N. Zhang, M. He, B. Chen and B. Hu, Simultaneous speciation analysis of inorganic arsenic, chromium and selenium in environmental waters by 3-(2-aminoethylamino) propyltrimethoxysilane modified multi-wall carbon nanotubes packed microcolumn solid phase extraction and ICP-MS, *Talanta*, 2015, **131**, 266–272.
15 S. Barua, I. M. M. Rahman, I. Alam, M. Miyaguchi, H. Sawai, T. Maki and H. Hasegawa, Liquid electrode plasma-optical emission spectrometry combined with solid-phase preconcentration for on-site analysis of lead, *J. Chromatogr. B*, 2017, **1060**, 190–199.
16 I. M. M. Rahman, Y. Furusho, Z. A. Begum, N. Izatt, R. Bruening, A. Sabarudin and H. Hasegawa, Separation of lead from high matrix electroless nickel plating waste solution using an ion-selective immobilized macrocycle system, *Microchem. J.*, 2011, **98**, 103–108.
17 S. M. Taghdisi, N. M. Danesh, P. Lavaee, M. Ramezani and K. Abnous, An aptasensor for selective, sensitive and fast detection of lead(II) based on polyethyleneimine and gold nanoparticles, *Environ. Toxicol. Pharmacol.*, 2015, **39**, 1206–1211.
18 L. Zhao, W. Gu, C. Zhang, X. Shi and Y. Xian, In situ regulation nanoarchitecture of Au nanoparticles/reduced graphene oxide colloid for sensitive and selective SERS detection of lead ions, *J. Colloid Interface Sci.*, 2016, **465**, 279–285.
19 S. Dadfarnia, A. M. Salmanzadeh and A. M. H. Shabani, A novel separation/preconcentration system based on solidification of floating organic drop microextraction for determination of lead by graphite furnace atomic absorption spectrometry, *Anal. Chim. Acta*, 2008, **623**, 163–167.
20 E. Efe and M. Imamoglu, Solid-phase extraction (SPE) of Ni(II), Cd(II) and Pb(II) ions using pyromellitic dianhydride functionalized silica gel prior to flame atomic absorption spectrometric determination, *Desalin. Water Treat.*, 2024, **317**, 100158.

 © 2026 The Author(s). Published by the Royal Society of Chemistry

Open Access Article. Published on 12 September 2025. Downloaded on 1/16/2026 10:05:29 AM.
This article is licensed under a Creative Commons Attribution-NonCommercial 3.0 Unported Licence.

21 V. Kumar, S. K. Dwivedi and S. Oh, A critical review on lead removal from industrial wastewater: Recent advances and future outlook, *J. Water Process Eng.*, 2022, **45**, 102518.
22 A. Murray and B. Örmeci, Use of polymeric sub-micron ion-exchange resins for removal of lead, copper, zinc, and nickel from natural waters, *J. Environ. Sci.*, 2019, **75**, 247–254.
23 R. Ram, L. Morrisroe, B. Etschmann, J. Vaughan and J. Brugger, Lead (Pb) sorption and co-precipitation on natural sulfide, sulfate and oxide minerals under environmental conditions, *Miner. Eng.*, 2021, **163**, 106801.
24 F. C. Rosa, F. A. Duarte, J. N. G. Paniz, G. M. Heidrich, M. A. G. Nunes, E. M. M. Flores and V. L. Dressler, Dispersive liquid–liquid microextraction: An efficient approach for the extraction of Cd and Pb from honey and determination by flame atomic absorption spectrometry, *Microchem. J.*, 2015, **123**, 211–217.
25 P. Sarker, M. Marumoto, I. M. M. Rahman, K. H. Wong, A. S. Mashio, T. Nishimura, K. Maeda and H. Hasegawa, Selective extraction of lead from chelator-rich effluents using a biomass-based sorbent, *Chem. Eng. J.*, 2024, **500**, 156831.
26 I. M. M. Rahman, Z. A. Begum and H. Hasegawa, Selective separation of elements from complex solution matrix with molecular recognition plus macrocycles attached to a solid-phase: A review, *Microchem. J.*, 2013, **110**, 485–493.
27 D. Prabhakaran and M. S. Subramanian, Selective extraction and sequential separation of actinide and transition ions using AXAD-16-BTBED polymeric sorbent, *React. Funct. Polym.*, 2003, **57**, 147–155.
28 D. Prabhakaran and M. S. Subramanian, A new chelating sorbent for metal ion extraction under high saline conditions, *Talanta*, 2003, **59**, 1227–1236.
29 J. P. Bernal, E. R. De San Miguel, J. C. Aguilar, G. Salazar and J. De Gyves, Adsorption of metallic cations on silica gel-immobilized 8-hydroxyquinoline, *Sep. Sci. Technol.*, 2000, **35**, 1661–1679.
30 A. O. Martins, E. L. da Silva, M. C. M. Laranjeira and V. T. de Fávere, Application of chitosan functionalized with 8-hydroxyquinoline: Determination of lead by flow injection flame atomic absorption spectrometry, *Mikrochim. Acta*, 2005, **150**, 27–33.
31 A. Sabarudin, N. Lenghor, Y. Liping, Y. Furusho and S. Motomizu, Automated online preconcentration system for the determination of trace amounts of lead using Pb-selective resin and inductively coupled plasma–atomic emission spectrometry, *Spectrosc. Lett.*, 2006, **39**, 669–682.
32 I. M. M. Rahman, Z. A. Begum, M. Nakano, Y. Furusho, T. Maki and H. Hasegawa, Selective separation of arsenic species from aqueous solutions with immobilized macrocyclic material containing solid phase extraction columns, *Chemosphere*, 2011, **82**, 549–556.
33 H. Hasegawa, I. M. M. Rahman, S. Kinoshita, T. Maki and Y. Furusho, Non-destructive separation of metal ions from wastewater containing excess aminopolycarboxylate chelant in solution with an ion-selective immobilized macrocyclic material, *Chemosphere*, 2010, **79**, 193–198.
34 R. M. Izatt, S. R. Izatt, N. E. Izatt, K. E. Krakowiak, R. L. Bruening and L. Navarro, Industrial applications of molecular recognition technology to separations of platinum group metals and selective removal of metal impurities from process streams, *Green Chem.*, 2015, **17**, 2236–2245.
35 R. M. Izatt, J. S. Bradshaw, R. L. Bruening, B. J. Tarbet and M. L. Bruening, Solid phase extraction of ions using molecular recognition technology, *Pure Appl. Chem.*, 1995, **67**, 1069–1074.
36 M. Hattori, Y. Takaku and T. Shimamura, Novel rapid separation of lead using highly selective resin for measurement of precise lead isotope ratio and its application to geochemical reference samples (In Japanese), *Bunseki Kagaku*, 2008, **57**, 113–121.
37 P. N. Nge, C. I. Rogers and A. T. Woolley, Advances in microfluidic materials, functions, integration, and applications, *Chem. Rev.*, 2013, **113**, 2550–2583.
38 A. Feng, N. T. Tran, C. Chen, J. Hu, M. Taverna and P. Zhou, In-line coupling SPE and CE for DNA preconcentration and separation, *Electrophoresis*, 2011, **32**, 1623–1630.
39 P. N. Nge, J. V. Pagaduan, M. Yu and A. T. Woolley, Microfluidic chips with reversed-phase monoliths for solid phase extraction and on-chip labeling, *J. Chromatogr. A*, 2012, **1261**, 129–135.
40 Y. Duan, H. Liu, S. Sun, Y. Gu, J. Li and G. Yang, On-line solid-phase extraction based on poly (NIPAAm-MAA-co-EDMA) monolith coupled with high-performance liquid chromatography for determination of nitrendipine and nisoldipine in human urine, *J. Chromatogr. Sep. Tech.*, 2012, **3**, 1–5.
41 L. Nováková and H. Vlčková, A review of current trends and advances in modern bio-analytical methods: Chromatography and sample preparation, *Anal. Chim. Acta*, 2009, **656**, 8–35.
42 J. Haginaka, Molecularly imprinted polymers as affinity-based separation media for sample preparation, *J. Sep. Sci.*, 2009, **32**, 1548–1565.
43 S. Kumar, V. Sahore, C. I. Rogers and A. T. Woolley, Development of an integrated microfluidic solid-phase extraction and electrophoresis device, *Analyst*, 2016, **141**, 1660–1668.
44 T. Ariga, T. Narukawa, H. Shu, S. Miyashita, I. Kudo, M. Oguchi and K. Inagaki, Development of NMIJ CRM 7202-c, a certified river water reference material for hazardous metal analysis (In Japanese), *Bunseki Kagaku*, 2020, **69**, 11–23.
45 G. Sharma, A. Tara and V. D. Sharma, Advances in monolithic silica columns for high-performance liquid chromatography, *J. Anal. Sci. Technol.*, 2017, **8**, 16.
46 R. Miyamoto, K. Kanamori, H. Nakagawa, H. Tanaka and H. Kaji, Significant waste reduction in liquid chromatography by a reusable large-volume monolithic silica column, *ACS Sustainable Chem. Eng.*, 2024, **12**, 6509–6518.
47 K. Shimizu, H. Kuribayashi, H. Watanabe, T. Shimasaki, K. Azuma, Y. Horie, K. Saitoh, S. Saito and M. Shibukawa,

Open Access Article. Published on 12 September 2025. Downloaded on 1/16/2026 10:05:29 AM.
This article is licensed under a Creative Commons Attribution-NonCommercial 3.0 Unported Licence.

Multistep pH-peak-focusing countercurrent chromatography with a polyethylene glycol-Na_2SO_4 aqueous two phase system for separation and enrichment of rare earth elements, *Anal. Chem.*, 2013, **85**, 978–984.

48 X. Zhang, B. Wang and J. Chang, Adsorption behavior and solidification mechanism of Pb(II) on synthetic C-S-H gel with low and high Ca/Si ratios in highly alkaline environments, *J. Environ. Chem. Eng.*, 2024, **12**, 113871.

49 V. Camel, Solid phase extraction of trace elements, *Spectrochim. Acta, Part B*, 2003, **58**, 1177–1233.

50 H. Hasegawa, I. M. M. Rahman, M. Nakano, Z. A. Begum, Y. Egawa, T. Maki, Y. Furusho and S. Mizutani, Recovery of toxic metal ions from washing effluent containing excess aminopolycarboxylate chelant in solution, *Water Res.*, 2011, **45**, 4844–4854.

51 M. Lo Irene and W. Zhang, Study on optimal conditions for recovery of EDTA from soil washing effluents, *J. Environ. Eng.*, 2005, **131**, 1507–1513.

52 J. Qi, X. He and Q. Lu, Novel chelating polyacrylonitrile membrane for efficient capture of Cu^{2+}, Pb^{2+} and Fe^{3+}, *Chem. Eng. J.*, 2022, **450**, 138203.

53 C. Yu, Q. Cai, Z.-X. Guo, Z. Yang and S. B. Khoo, Inductively coupled plasma mass spectrometry study of the retention behavior of arsenic species on various solid phase extraction cartridges and its application in arsenic speciation, *Spectrochim. Acta, Part B*, 2003, **58**, 1335–1349.

54 T. Ikegami and N. Tanaka, Monolithic columns for high-efficiency HPLC separations, *Curr. Opin. Chem. Biol.*, 2004, **8**, 527–533.

55 J. S. Bradshaw, R. L. Bruening, K. E. Krakowiak, B. J. Tarbet, M. L. Bruening, R. M. Izatt and J. J. Christensen, Preparation of silica gel-bound macrocycles and their cation-binding properties, *J. Chem. Soc., Chem. Commun.*, 1988, 812–814.

56 M. Rahm, R. Hoffmann and N. W. Ashcroft, Atomic and ionic radii of elements 1–96, *Chem.–Eur. J.*, 2016, **22**, 14625–14632.

57 R. D. Shannon, Revised effective ionic radii and systematic studies of interatomic distances in halides and chalcogenides, *Acta Crystallogr., Sect. A*, 1976, **32**, 751–767.

58 K. P. Gregory, G. R. Elliott, H. Robertson, A. Kumar, E. J. Wanless, G. B. Webber, V. S. J. Craig, G. G. Andersson and A. J. Page, Understanding specific ion effects and the Hofmeister series, *Phys. Chem. Chem. Phys.*, 2022, **24**, 12682–12718.

59 W. J. Xie and Y. Q. Gao, A Simple Theory for the Hofmeister Series, *J. Phys. Chem. Lett.*, 2013, **4**, 4247–4252.

60 W. Kunz, J. Henle and B. W. Ninham, 'Zur Lehre von der Wirkung der Salze' (about the science of the effect of salts): Franz Hofmeister's historical papers, *Curr. Opin. Colloid Interface Sci.*, 2004, **9**, 19–37.

61 Y. Marcus, Effect of Ions on the Structure of Water: Structure Making and Breaking, *Chem. Rev.*, 2009, **109**, 1346–1370.

62 K. H. Stern and E. S. Amis, Ionic size, *Chem. Rev.*, 1959, **59**, 1–64.

63 Y. Marcus, Ionic radii in aqueous solutions, *Chem. Rev.*, 1988, **88**, 1475–1498.

64 M. Thomas Record, W. Zhang and C. F. Anderson, in *Adv. Protein Chem.*, ed. E. Di Cera, Academic Press, 1998, vol. 51, pp. 281–353.

65 K. D. Collins and M. W. Washabaugh, The Hofmeister effect and the behaviour of water at interfaces, *Q. Rev. Biophys.*, 1985, **18**, 323–422.

66 H. Hasegawa, I. M. M. Rahman, Z. A. Begum, Y. Umehara, T. Maki, Y. Furusho and S. Mizutani, A silica gel-bound macrocycle system for the selective separation of toxic cadmium from metal-affluent aqueous matrix, *Cent. Eur. J. Chem.*, 2013, **11**, 341–347.

67 L. González-Rodríguez, Y. Hidalgo-Rosa, J. O. P. García, M. A. Treto-Suárez, K. Mena-Ulecia and O. Yañez, Study of heavy metals adsorption using a silicate-based material: Experiments and theoretical insights, *Chem. Phys. Impact*, 2024, **9**, 100714.

68 X. Ma, H. Sun and P. Yu, A novel way for preparing high surface area silica monolith with bimodal pore structure, *J. Mater. Sci.*, 2008, **43**, 887–891.

 © 2026 The Author(s). Published by the Royal Society of Chemistry